Vol 11 No 8, August 2002
1009-1963/2002/11(08)/0776-09

Chinese Physics

© 2002 Chin. Phys. Soc.
and IOP Publishing Ltd

Lipid membrane: inelastic deformation of surface structure by an atomic force microscope*

Zhang Jing(张 静)† and Sun Run-Guang(孙润广)

Department of Food Engineering, College of Physics and Information Technology and Shaanxi Normal University 710062 *Xi'an, China*

(Received 21 October 2001; revised manuscript received 21 March 2002)

The stability of the 1,2-Dioleoyl-sn-Glycero-3-[phospho-rac-1-Glycerol-Na] liposome in the liquid crystalline state have been investigated using an atomic force microscope (AFM). We have observed the inelastic deformation of the sample surface. The AFM tip causes persistent deformation of the surface of the lipid membrane, in which some of the lipid molecules are eventually pushed or dragged by the AFM tip. The experiment shows how the surface structure of the lipid membrane can be created by the interaction between the AFM tip and lipid membrane. When the operating force exceeds 10^{-8} N, it leads to large deformations of the surface. A square region of about $1 \times 1\mu m^2$ is created by the scanning probe on the surface. When the operating force is between 10^{-11}N and 10^{-8}N, it can image the topography of the surface of the lipid membrane. The stability of the sample is related to the concentration of the medium in which the sample is prepared.

Keywords: atomic force microscope, lipid bilayers, liquid crystalline state
PACC: 0779, 8720, 6130

1. Introduction

The atomic force microscope (AFM) is a powerful tool for studying biological samples.[1−7] It can be used to image the surface of both conductors and nonconductors even if they are covered with water or aqueous solutions.[8−12] It has been used in a variety of surface studies including atomic scale friction, elasticity and surface forces. Not only can the AFM be used for imaging the topography of the surfaces, but it can also be used for measuring forces on the molecular level, while the operating force between the AFM tip and the surface molecules can be exploited for the creation of a structure on a nanometre scale. It is an interesting and attracting subject to understand the atomistic mechanisms of interaction between the AFM tip and molecules of the sample surface in the lipid membrane spread on silicon wafers.[13,14]

Langman *et al*[15] have shown how the interaction between the Ni tip and Au surface in an AFM creates an atomic scale instability that pulls Au atoms towards Ni, eventually coating the tip. While moving the sample towards and away from the tip repeatedly along the Z-direction and monitoring the cantilever deflection, the operating force can be measured by holding the cantilever stationary. In the experiment by Leung and Goh,[13] the polymer molecules forming the surface film were entangled through their long chains. The deformation produced by the tip–surface interaction in this case is apparently long-lived. Later, Singh and Keller[2] have shown the result of their experiment to see how the membrane was damaged by the AFM tip. In the course of the deformation, different configurations of the polymer chains have been generated, resulting in a surface structure that can be kept for a long time. In a recent report, Maas *et al*[16] have shown that the AFM tip produces rims on a microscopic scale, oriented perpendicular to the scanning direction. Scanning the area in between two rims has shown that there is no polymer left on the surface. In these investigations, one monitors the deflection of the AFM tip, caused by its interaction with the surface on which a scan is made, to map out the surface topography. In this paper, we specifically investigate the 1,2-Dioleoyl-sn-Glycero-3-[phospho-rac-1-Glycerol-Na] (DOPG-Na) membrane made by the

*Project supported by the National Natural Science Foundation of China (Grant No 29672024) and the Foundation for University Key Teachers by the Ministry of Education, China (Grant No 2000-65)

†To whom correspondence should be addressed: Professor Dr Run Guang Sun and Jing Zhang, Shaanxi Normal University, PO Box 27-3-18, 710062 Xi'an, China. E-mail: sunrun@pub.xaonline.com or sunrunguang@netscape.net

adsorption of DOPG-Na on to a flat silicon surface. We also investigate how the surface structure and elastic behaviour of the DOPG-Na membrane in the liquid crystalline state changes when the AFM tip scans the surface of the adsorbed lipid membrane. The results of our study show how interesting surface structures can be created by the interaction between the AFM tip and the lipid membrane.

2.Materials and methods

2.1. Materials

DOPG-Na (Sigma Chemical Co.) was obtained commercially and used without further purification. All the organic and inorganic chemicals—glucose, sucrose, NaCl, KCl, chloroform and methanol—were of analytical reagent grade, purchased from Xi'an or Shanghai Chemical Reagent Company in China, and were also used without further purification. The water used was deionized (NANO pure water, Barn-stead, Iowa, USA).

2.2. Method of lipid vesicle preparation

The lipids were first dissolved and mixed in an organic solvent. This process was carried out using chloroform:methanol (3/1 v/v) mixtures. Typically, lipid solutions were prepared in a 10–20mg lipid/ml organic solvent. To yield a lipid film, the solvent was evaporated using nitrogen in a fume hood. Then, hydration of the lipid membrane was accomplished simply by adding an aqueous medium into the container of lipid and agitating. The temperature of the hydrating medium should be above the gel–liquid crystal transition temperature T_c of the lipid (T_c=–18°C). After the addition of the hydrating medium (0.9wt% salt solution: NaCl 1M; 0.1M; 0.01M, 0.001M, respectively, 5wt% glucose, and 10wt% sucrose), the round-bottom flask was spun while maintaining a temperature above the T_c of the lipid suspension. After hydration for 1 h with vigorous shaking and mixing, the lipid suspension was forced through a filter with a definite pore size to yield particles with a diameter near the pore size of the filter used. Extrusion through filters with 200nm pores is typical.

2.3. Methods of AFM measurements

Silicon wafers with an oxide layer of approximately 80 nm, prepared by thermal oxidation, thin layer were used as substrates. Thin DOPG-Na layers were prepared by spin-coating from an adsorbed layer concentrated solution (20mg/mL) of DOPG-Na. In order to obtain an adsorbed layer, the excess material was removed by washing with fresh solvent. Finally, samples were dried with nitrogen. The thickness of the layers was determined by computer-controlled null ellipsometry (Sentech SE-400). The refractive index for λ=632.8nm was taken to be 1.4584. The AFM measurements were performed with a Digital Instruments Nanoscope III AFM equipped with a scanner capable of scanning an area of 12μm×12μm. All the measurements were performed at room temperature and at a relative humidity of 50–60%. Commercially available Si_3N_4 tips were used on cantilevers with a spring constant of approximately 0.58N/m.

2.4. Data analysis of the force curves

Elastic force leads to the indentation curve on an elastic sample. The slope of a force curve gives the elastic properties of a sample in a qualitative way. In the case of a very hard sample, the displacement z of the piezo-device during contact will lead to a deflection d of the cantilever that is identical to z, i.e. d=z. In the case of a soft sample, the cantilever tip will indent the sample. This indentation δ leads to a smaller deflection $d = z - \delta$, resulting in a flatter force curve with a smaller slope. The loading force F is proportional to the deflection d of the cantilever and the spring constant k_H of the cantilever and can be written as (Hooke's law)

$$F_{\text{elastic}} = -k_H d = k_H(z - \delta). \qquad (1)$$

In a force curve we measure the deflection as a function of z of the piezo-device. Equation (1) can be used to calculate indentation versus force from the measured data. The indentation versus force curve can then be analysed by modelling the elastic indentation by Eq.(1), as discussed below.

To describe the elastic deformation of two surfaces touching each other under a loading force, we model the force versus indentation curves using the Hertz model. Two different geometries seem to be appropriate to describe the AFM tip and the sample: either a sphere of radius R or a cylindrical cone of a vertex angle α indenting a planar soft sample. For these two cases, the Hertz model predicts different functional relations between the loading force and the indentation.

2.4.1. Spherical indentation for the Hertz model

For an infinitely hard sphere, the model gives the following relation between the loading force F and the indentation δ

$$F_s = \frac{4E\sqrt{R}}{3(1-\nu^2)}\delta^{3/2}, \tag{2}$$

where E is Young's modulus and ν is the Poisson ratio.[13] For an infinitely hard sphere of radius R touching a soft planar surface, to calculate Young's modulus, we use a fit of the Hertz model to the experimental curve calculated as the average value of the approaching and retracting traces of each force curve. Combining Eqs.(1) and (2) yields

$$z - z_0 = d - d_0 + \sqrt[3]{\frac{k_H^2(d-d_0)^2}{(4/3)^2[E^2/(1-\nu^2)^2R]}}, \tag{3}$$

where z_0 and d_0 are the offsets of the sample height and the deflection, respectively, The offset of the deflection d_0 can easily be determined by calculating the mean deflection at the very beginning of the force curves (typically the first 100nm), where the cantilever is off the surface. Determining the offset of the sample height is easy with force curves on stiff substrates, but it is more difficult with the force curves on the soft samples because they do not show a sharp kink in the deflection.

2.4.2. Cylindrical indent for the Hertz model

In the case of a cylindrical cone indenting a soft material, the relationship between the loading force and the resulting indentation is as follows

$$F_{\text{cone}} = \frac{\pi}{2}\frac{E}{(1-\nu^2)}\tan(\alpha)\delta^2, \tag{4}$$

where α is the vertex angle of the cone. In the following, we show which model is more appropriate in our cases. The two functions (3) and (4) appear as lines with different slopes on a log–log plot. In the case of a cylindrical cone indenting a soft material, to calculate Young's modulus, we apply a fit of the Hertz model to the experimental curve calculated as the average value of the approaching and retracting traces for each force curve. Combining Eqs.(1) and (4) yields

$$z - z_0 = d - d_0 + \sqrt{\frac{k_H(d-d_0)}{(\pi/2)[E^2/(1-\nu^2)]\tan\alpha}}. \tag{5}$$

Unfortunately, Eq.(5) is in such a form that an analytical least-squares fit to determine the two fit parameters E and z_0 cannot be obtained. A possible alternative would be to do a Monte Carlo fit with reasonable starting values. It turns out that the signal-to-noise ratio of the measured data is very good, so that the two parameters can be obtained easily. It is necessary to take only two height values with their corresponding deflection values and enter them in the equation. These two data points set up equations that can be inverted to obtain values for the elastic modulus E and the offset z_0 of the height. The fitted data shown below are determined by this method, which show the quality of this very simple fit method. In Fig.1, the force curves for the lipid films are taken at different NaCl concentrations. We use 0.58N/m as the determined force constant and 17° as the half-vertex angle of the cone, according to the specifications of the manufacturer. We assume a Poisson ratio of 0.5. Calculations indicate that Young's modulus is of the order of 10^6N/m^2, in good agreement with the published data.[4]

2.4.3. Calculation of Young's modulus

The quantities to be used can be determined independently by taking two different deflection values and their corresponding z values from a force curve. These two data points then define the range of deflection values, and the average data of the approaching and retracting traces are plotted. Young's modulus is obtained as follows:

$$\frac{k_H(d_2-d_1)}{\left(\frac{\pi}{2}\right)\left(\frac{E}{1-\nu^2}\right)\tan\alpha} = [(z_2-z_1)-(d_2-d_1)]^2. \tag{6}$$

If $z_2 - z_1 = A$, $d_2 - d_1 = B$, then

$$\left(\frac{\pi}{2}\right)\left(\frac{E}{1-\nu^2}\right)\tan\alpha = \frac{k_H B}{(A-B)^2}, \tag{7}$$

$$E = \left(\frac{2}{\pi}\right)\left(\frac{k_H B(1-\nu^2)}{(A-B)^2\tan\alpha}\right). \tag{8}$$

Young's modulus is listed in Table 1.

Table 1. Different ranges of the applied Hertz model and respective Young's modulus for the lipid bilayer.

Range of analysis cantilever deflection, nm	Calculated Young's modulus, N/m^2
5–10	1.133×10^6
10–15	1.812×10^6
15–20	7.245×10^6
20–25	7.245×10^6
25–30	7.245×10^6
30–35	7.245×10^6
35–40	7.245×10^6

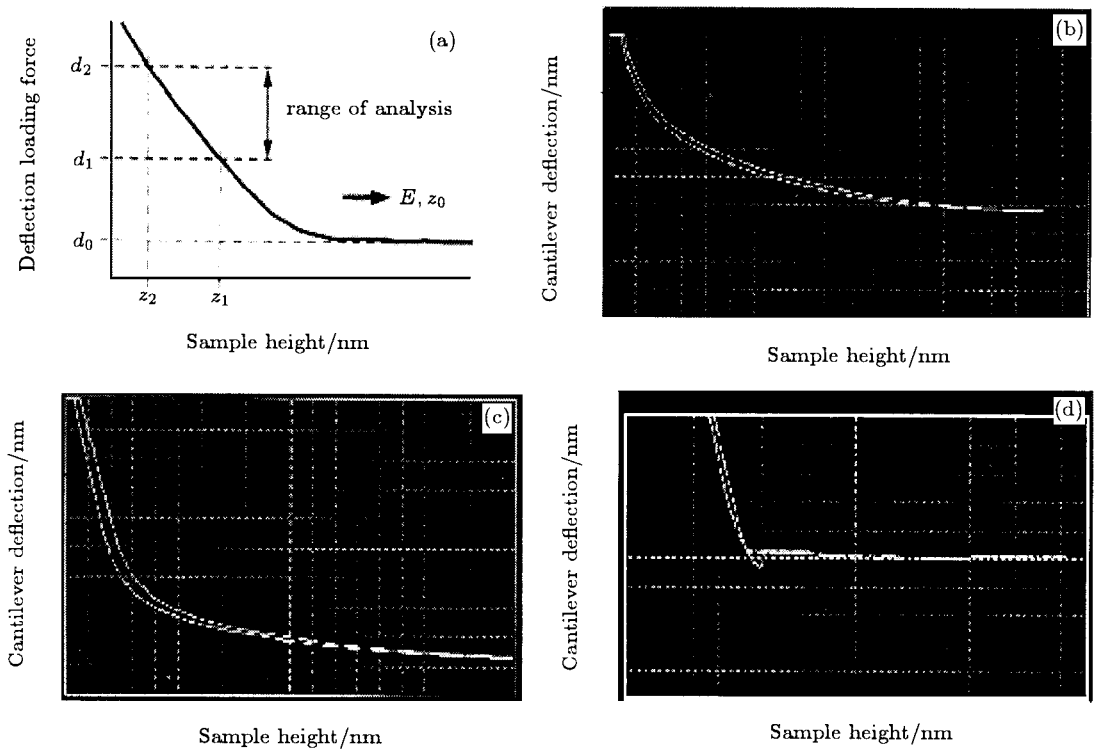


Fig.1. (a) Force curve on a lipid film. The average data of the approaching and retracting traces are plotted. Parameters necessary for data analysis are depicted in the graph: the zero deflection (force) d_0 and the range of analysis defined by the two data points $(d_1,\ z_1)$ and $(d_2,\ z_2)$. The analysis as described in the text yields independently the contact point z_0 and Young's modulus E. Force curves on the lipid film are taken at different NaCl concentrations. Here, we see that these curves are highly nonlinear because of elastic indentation. (b) 10mmol/L NaCl, (c) 100mmol/L NaCl and (d) 1000mmol/L NaCl.

3. Experimental results

3.1. Scratching the corrugated membrane in a contact mode

Molecular dynamics and an AFM have been used to investigate the mechanisms of adhesion, contact formation, nano-indentation, separation and fracture that occur when the AFM tip interacts with the surface of the samples.[13,16] In our experiment, using a novel tapping mode, we did not obtain the images of deformations of the surface in liquid crystals (Fig.2(a)). In the conventional contact mode, theoretical calculations indicate that forces of the order of 10^{-8}N can lead to large deformations of the surface.[17–19] We have proven that the operating force should lie between 10^{-11}N and 10^{-8}N for biological samples. When the operating force exceeds 10^{-8}N, it can lead to large deformations of the surface. When the operating forces lie between 10^{-11}N and 10^{-8}N, the operating force reveals the topography of the lipid membrane. We have investigated the case when the electric and elastic force existing between the AFM tip creates a structure of the order of nanometres to micrometres. Our experiment shows that the approaching and subsequent separation of the AFM tip from the surface of the lipid membranes causes inelastic deformation of the sample surface. When one attempts to image the adsorption on the surface with an AFM, at small tip–sample distances, the mechanical instability causes the AFM tip to jump to contact with the surface. As the sample is brought closer to the AFM tip, the interaction increases.[20] The process of scanning can drag or push molecules around the tip and lead to the distortion or disappearance of images. Subsequent indentation of the substrate results in the onset of persistent deformation of the lipid membranes. The results of our study show how surface structures can be created by the interaction between the AFM tip and the lipid membranes.

In Fig.2(b), scanning the scratch and crinkle in the tapping mode over an area of $1 \times 1\mu\text{m}^2$ shows that there are some ridges and grooves on the surface of the adsorbed layer, forming smaller or larger corrugations in the area. This indicates that the membranes are pulled off from the surface by the AFM tip. The re-

sult shows that the membranes of DOPG-Na vesicles are damaged by the AFM tip.

In the height image, the sample surface is seen as a pattern with alternative bright and dark regions (Fig.2(b)). The bright bands can be assigned to the creased ridges. The darker patches are depressed regions like furrows. The difference in height between the bright and dark areas is about 10 nm. It is obvious that there is a huge difference in the average distance between the ridge and the furrow. The average distance is not only a function of the fraction of DOPG-Na vesicles, but also depends on the total length of the DOPG-Na molecule.[8,11] The overall pictures are captured by the scan. Scratching the membrane with the AFM tip at high force and high frequency shows that no lipids are left between two ridges. The observation suggests that the DOPG-Na membranes can be creased and the surface is pulled off easily. Our experiments show that the DOPG-Na membrane can be swept into ridges and furrows over the silicon surface.

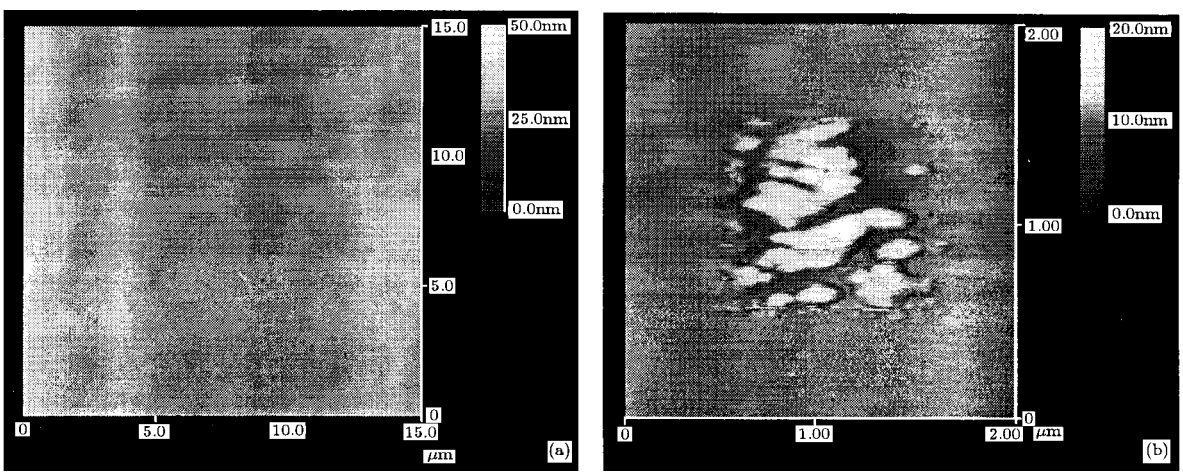


Fig.2. (a) AFM images were taken in novel tapping mode in the liquid crystalline state. In our experiment, we did not obtain images of the deformations of the surface in the tapping mode in liquid crystals. (b) When a large area of $2 \times 2\mu m^2$ was scanned for 30 min, a small region in the centre was scanned and smaller and larger corrugations can been seen. Scanning the scratch and crinkle in the contact mode shows that there are some ridges and grooves on the surface of the adsorbed layers forming smaller and larger corrugations in the square region of $1 \times 1\mu m^2$ in the centre. The result of the experiment shows that the membranes of adsorbed DOPG-Na vesicles on silicon are damaged by the AFM probe.

In Fig.3(a), three square regions are created in the upper and lower centre by scanning the probe over the regions of the surface at relatively high, repulsive tip–sample force (~10nN more than normal) then lowering the force and widening the scan to view the damage.[2] It is possible to create roughened patches such as these as the inevitable outcome. When similar regions are scanned at high force for the same length of time and under the same conditions, the damaged membrane could occur, showing that the membrane of adsorbed DOPG-Na vesicles on silicon is not stable under imaging conditions. In fact, when the square regions in the centre are scanned at high force, they will be damaged.

A view of the damaged patches at higher magnification is captured by the scan in Fig.3(b). The sites of damage appear to be small patches in the membranes. Measurements of the small patches are consistent with the rips being one bilayers in thickness (5~6nm). Because the substrate is entirely coated with lipid, it is possible to tell using the AFM that there is a single layer or bilayers on the surface. Fig.3(b) shows the image of the sample in which the AFM probe has apparently damaged some of the lipid vesicles. In fact, the furrow created by the AFM tip is stable for subsequent imaging. We suggest that, under the present imaging conditions, the lipid vesicles have lamellar structures with a little water in their centres.

One of the main problems encountered in applying scanning probe microscopy to biological systems is the tendency of the latter being damaged or even entirely swept aside by the force between the AFM tip and the sample. The results of our experiment show that the damages are caused by scanning the adsorbed membrane at high force, and suggests that the occasional damage to DOPG-NA vesicles, under normal imaging conditions, are caused by the AFM tip which

is too near the damaged point.

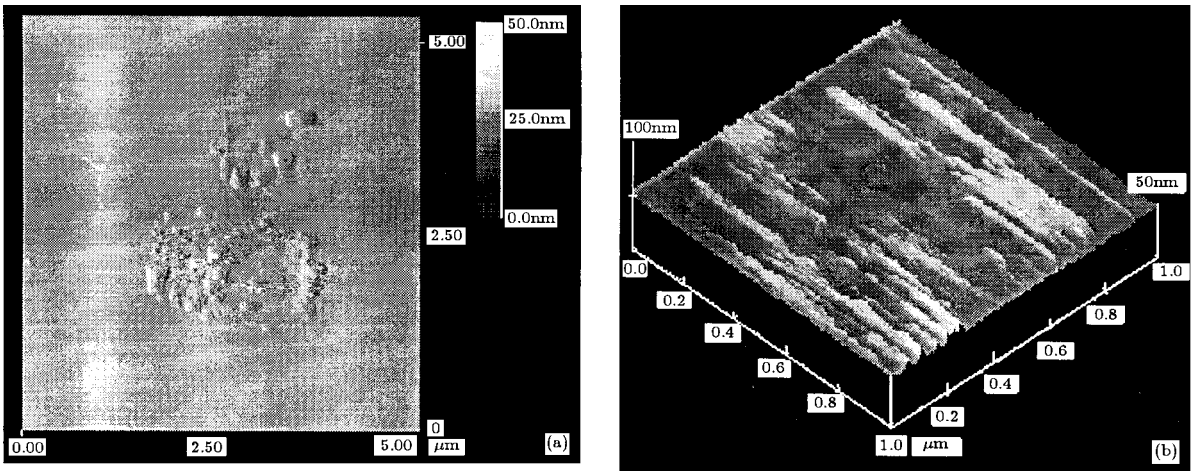


Fig.3. (a) The results of the experiment show that the lipid membranes are damaged by the AFM tip. The three square, roughened patches in the upper and lower centre are created in the originally uniform membrane by scanning at high force for an extended period. (b) The damaged patches of the membrane are consistent with the rips being of thickness 5–6nm.

3.2. Deformation of the lipid membrane by tip–surface interaction

Biological compounds can be imaged when they are attached to a silicon surface. The lipids, DOPG-Na, were dissolved in 75% chloroform–25% methanol at a concentration of 20mg/ml. The solvent was evaporated using nitrogen. The hydrating medium (0.9wt% salt solvent, 5wt% glucose and 10wt% sucrose) was then added. Lipid suspension was forced through a filter. Thin DOPG-Na membranes were prepared. In order to obtain the adsorbed membrane, excess material was removed by washing with fresh solvent. As mentioned above, the DOPG-Na molecules adhered to the silicon surface. The sample was put into an AFM. It is not only possible to image lipid membranes, but also to monitor the stability and deformational processes of the lipid membrane. In this paper, we present images of the DOPG-Na membranes. It is perhaps an important model system for demonstrating lipid membrane stability by the AFM tip–surface interaction.

Firstly, we imaged the surface for a few minutes and see fleeting images of the DOPG-Na molecules. We then investigated the effect of moving the AFM tip slowly across the surface. Finally, we took images of the lipid membrane as a function of time while scanning continuously and maintaining a constant force. The image taken immediately after deposition and solvent evaporation shows that the surface coverage is homogeneous and smooth. When the sample surface is scanned with the AFM, the AFM tip starts to pull the lipid membrane off the surface. The total amount of lipid molecules collected by the tip increases until the tip–lipid adhesion reaches a critical level. As the AFM tip provides a limited area of adhesion, the stress at the tip increases and, at a certain critical stress, the AFM tip jumps over the collected lipid. Then, the process starts again and the AFM tip jumps over the second creased ridge. This process is repeated. After a few minutes, the roughness of the surface has increased in width (d) and thickness (z). With further scanning, these structures are better defined and increase in width and thickness. At this point, there appear to be distinctly formed smaller and larger corrugations in the square region. The increase in surface roughness and the formation of distinct corrugation is shown more clearly in Fig.4. It indicates how the AFM tip produces persistent deformation on the lipid membrane.

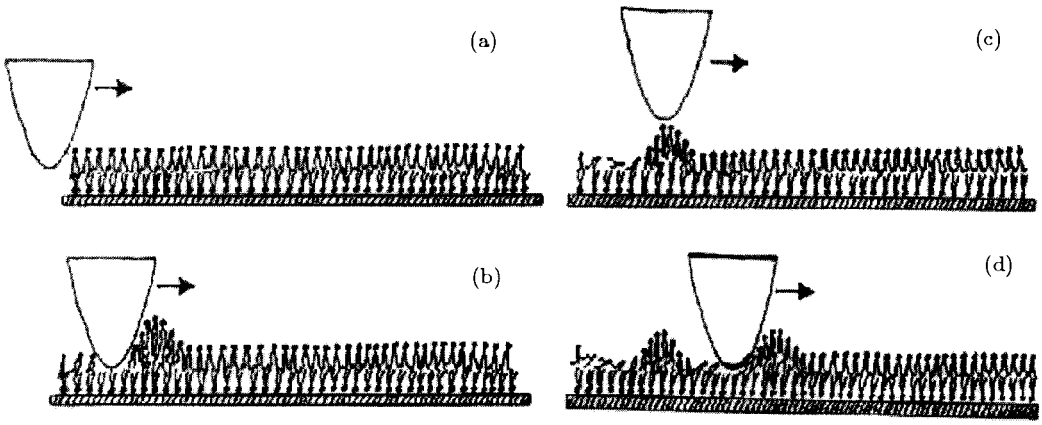


Fig.4. The AFM can image stability and deformational processes of the lipid membrane. (a) The AFM tip starts to pull the lipid membrane off the surface, (b) the stress at the AFM tip increases, (c) the AFM tip jumps over, (d) the process starts again and the AFM tip jumps over the second creased ridge.

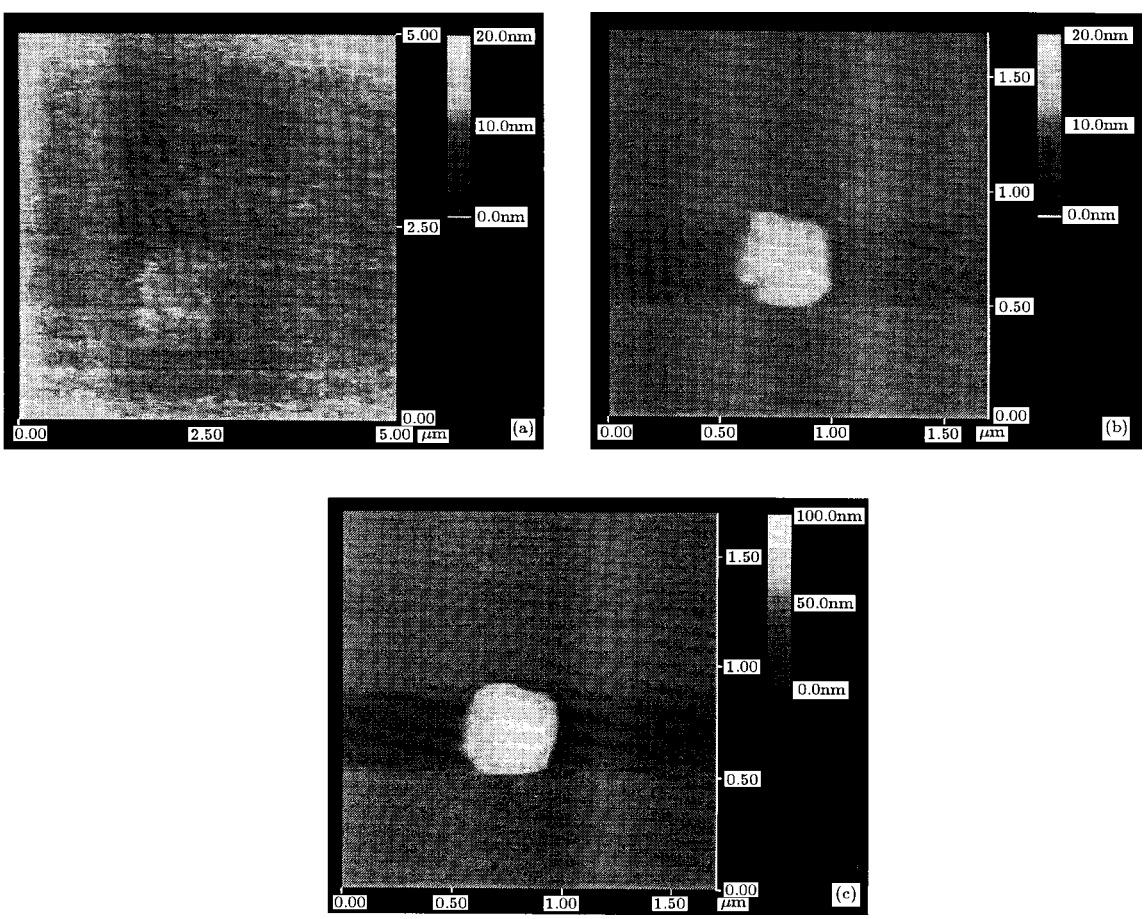


Fig.5. The DOPG-Na vesicles form bilayers or multi-layers for preparation at 1mol/L NaCl solution (a), in glucose (b) and in sucrose solutions (c). The images of deformations of the surface were obtained from the interaction between the tip of the AFM and the surface of the DOPG-Na film.

3.3. Effect of electric interaction on the stability of the lipid membrane

We have investigated the effects of electric interaction on the stability and surface structure of DOPG-Na vesicles. When the DOPG-Na vesicles are prepared in NaCl solutions, their bilayer membranes are more stable with increasing NaCl concentration. This can be seen as the AFM tip exerts force on the membrane of adsorbed lipid vesicles, which may form bilayers or multi-layers for preparation at 1mol/L NaCl (Fig.5(a)), and at low concentrations there is perma-

nent damage. For KCl it is just the opposite, The bilayer membranes prepared in KCl solutions are more stable with decreasing KCl concentration, and at high concentrations there is permanent deformation. We have also investigated the effects of glucose and sucrose respectively on the stability and surface structure of DOPG-Na vesicles. When DOPG-Na vesicles are prepared in glucose and sucrose solutions, they form stable bilayer membranes (Figs.5(b) and (c)).

4. Discussion

We have intentionally operated at comparatively large forces (in the vicinity of 10^{-8}N) to enhance the tip–surface interaction. The AFM tip can be positioned in one particular spot, a few nanometres above the sample. This distance should be sufficiently small, such that there is enough interaction to allow the AFM tip to track the topography of the sample. As the sample was brought closer to the AFM tip, the interaction was increased. We used this force mode of operation of the AFM to examine the interaction between the AFM tip and the bilayer membranes. After 10 min, the corrugation was about 20 nm high and 30 nm in diameter. The asymmetry of the corrugation possibly reflects the shape of the AFM tip. Obviously, it is the interaction between the AFM tip and the lipid membrane that causes the deformation of the surface. The experiment of Leung and Goh[13] has shown that there are two interesting aspects of the pattern of structures formed. They suggested that the polymer molecule could drag several chains with it, which in turn were likely to pull other chains, producing a lump in the surface. Singh and Keller[2] found that two square patches were created by scanning the probe over a patch of surface at relatively high, repulsive tip–sample force (∼10nN greater than normal). Recently, Maas *et al*[16] have shown that, in a small region in the centre which was scanned for 30 min, few and very large rims can been seen. Scanning the area in between two rims has shown that there is no polymer left on the surface. In these investigations, when one attempts to image adsorbed molecules on a surface with an AFM, the process of scanning can drag or push molecules around and lead to distorted or disappearing images. In our experiment, the main difference is that there are some ridges and grooves on the surface of the adsorbed layers of DOPG-Na, forming smaller and larger corrugations in the square region. This indicates that the membranes are pulled off the surface by the AFM tip. The result of the experiment shows that the membranes of adsorbed DOPG-Na vesicles on silicon are damaged by the AFM probe.

Leung and Goh[13] have suggested that three conditions are necessary for the formation of surface structures: (i) there must be a reasonable balance between tip–surface molecule forces versus surface molecule–surface molecule forces; (ii) the deformation should be plastic; and (iii) there must be enough molecules on the surface. Except for the above-mentioned conditions, we show that the following conditions are necessary for the deformation of surface structures by the tip–surface interaction. (i) The operating force should lie between 10^{-11}N and 10^{-8}N for biological samples. When the operating force exceeds 10^{-8}N, it can lead to large deformation of the surface. When the operating forces lie between 10^{-11}N and 10^{-8}N, the operating force leads to topographical changes of lipid membrane. (ii) A square region of about $1 \times 1\mu m^2$ is created by scanning the probe on the region for up to 30 min. (iii) The stability of the sample is related to the medium; for example, there is a stable effect of glucose and sucrose on bilayer membranes. We realize these conditions in our experiments by using lipid membrane deposited on to the surface as bilayer. The tip–surface interaction may be strong enough to cause the deformation of the surface under certain conditions. This indicates that the AFM is a powerful tool for studying the stability of biological samples.

References

[1] Manfred R, Monika F, Claudia M K, Jason P C and Paul K H 1996 *Biophys. J.* **70** 556

[2] Singh S and Keller D J 1991 *Biophys. J.* **60** 1401

[3] Sun R G, Zhang J and Qi H 2001 *Acta Biophys. Sin.* **17** 53 (in Chinese)

[4] Sun R G, Zhang J and Wang Y C 2000 *Prog. Biochem. Biophys.* **27** 296 (in Chinese)

[5] Sun R G, Zhang J, Dai Z H, Xu F X and Wang D H 1994 *Acta Phys. Sin.* **43** 616 (in Chinese)

[6] Sun R G, Zhang J, Wang D H, Wang F R and Wang Z H 1993 *Acta Phys. Sin.* **42** 360 (in Chinese)

[7] Zhang J and Sun R G 1994 *Acta Phys. Sin.* **43** 1495 (in Chinese)

[8] Sun R G, Wang D H, Wang Z H and Zhang J 1992 *Acta Phys. Sin.* **41** 554 (in Chinese)
[9] Sun R G, Zhang J and Wang Y C 1999 *Acta Biophys. Sin.* **15** 675 (in Chinese)
[10] Sun R G, Zhang J and Wang Y C 1998 *Sci. China* B **41** 1
[11] Drake B, Prater C B, Weisenhorn A L, Gould S A C, Albrecht T R, Quate C F, Cannell D S, Hansma H G and Hansma P K 1989 *Science* **243** 1586
[12] Lou S T 2001 *Chin. Phys.* **10** 108
[13] Leung O M M and Goh C 1992 *Science* **255** 64
[14] Yan L, Zhang Y P, Pen Y P, Pang S J and Gao H J 2001 *Acta Phys. Sin.* **50** 2132 (in Chinese)
[15] Langman U, Luedtke W D,Burnham N A and Colton R J 1990 *Science* **248** 454
[16] Maas J H, Cohen Stuart M A and Fleer G J 2000 *Thin Solid Films* **358** 234
[17] Abraham F F and Barra I P S 1989 *Surf. Sci.* **209** L125–32
[18] Mou J D, Yang J, Huang C and Shao Z F 1994 *Biochemistry* **33** 9981
[19] Person B N 1987 *Chem. Phys. Lett.* **54** 366
[20] Sun R G, Qi H and Zhang J 2002 *Acta Phys. Sin.* **51** 41 (in Chinese)